Journal of Low Temperature Physics, Vol. 138, Nos. 3/4, February 2005 (© 2005)
DOI: 10.1007/s10909-005-2263-6

Phase diagram of turbulence in superfluid ^{3}He-B

A.P. Finne[*], S. Boldarev[*,†], V.B. Eltsov[*,†], and M. Krusius[*]

[*] *Low Temperature Laboratory, Helsinki University of Technology, P.O. Box 2200, FIN-02015 HUT, Finland*
[†] *Kapitza Institute for Physical Problems, 119334 Moscow, Russia*

In superfluid ^{3}He-B mutual-friction damping of vortex-line motion decreases roughly exponentially with temperature. We record as a function of temperature and pressure the transition from regular vortex motion at high temperatures to turbulence at low temperatures. The measurements are performed with non-invasive NMR techniques, by injecting vortex loops into a long column in vortex-free rotation. The results display the phase diagram of turbulence at high flow velocities where the transition from regular to turbulent dynamics is velocity independent. At the three measured pressures 10.2, 29.0, and 34 bar, the transition is centered at $0.52-0.59\,T_c$ and has a narrow width of $0.06\,T_c$ while at zero pressure turbulence is not observed above $0.45\,T_c$.

PACS numbers: 47.37, 67.40, 67.57
Keywords: quantized vortex; turbulence; vortex dynamics; mutual friction

1. INTRODUCTION

According to the original Landau picture of superfluidity superflow is irrotational: $\boldsymbol{\nabla}\times\boldsymbol{v}_{\rm s}=0$. This condition severely restricts the possible motions of the superfluid: When placed in a rotating container, it cannot participate in rotation. Later Onsager and Feynman suggested the modern view of superfluid dynamics: By the creation of quantized vortex lines the superfluid is able to mimic arbitrary complex flows on length scales which are large compared to the inter-vortex spacing. It was discovered more than 40 years ago that if superfluid ^{4}He is driven sufficiently fast then a complex vortex tangle appears. This tangle produces apparently chaotic time-dependent flow at different length scales. Such motion was called superfluid or quantum turbulence.[1]

Studies of turbulence in a different superfluid, the B phase of super-

0022-2291/05/0200-0567/0

fluid ^{3}He, have started only recently.[2,3] From the hydrodynamics point of view ^{3}He-B differs from ^{4}He in two important respects. First, the viscosity of the normal component in ^{3}He-B is large compared to both the (sample size)×velocity in a typical experiment and to the circulation quantum. This means that the normal component of ^{3}He-B is always in well-defined externally imposed laminar motion, which considerably simplifies the analysis of the experimental results. Second, the damping of the superfluid motion varies significantly in ^{3}He-B as a function of temperature. Such damping comes from the interaction of the thermal quasiparticles with the cores of the quantized vortices (so-called mutual friction). The magnitude of the friction[4] changes from large values (typical for superconductors) in the limit $T \to T_c$ to small values (typical for ^{4}He-II) at temperatures $T < 0.5\,T_c$.

In a recent experiment[2] we discovered that there is a sharp transition in the character of superfluid motion in ^{3}He-B as a function of temperature at $P = 29$ bar pressure. When the laminar vortex-free superflow is prepared by rotation of the cylindrical sample and a few seed vortex loops are injected into it, then these loops expand in a regular manner, with their number conserved at $T \gtrsim 0.6\,T_c$ or, proliferate to a turbulent vortex tangle at $T \lesssim 0.6\,T_c$. (Eventually the turbulent tangle polarizes to mimic the global rotating flow of the normal component which compensates the driving force and the turbulence decays to a cluster of rectilinear lines containing $\sim 10^3$ vortices.)

The transition to turbulence is controlled by the mutual friction damping. It can be understood by analyzing the dynamic equation for the coarse-grained superfluid velocity $\boldsymbol{v}_s$ which is averaged over volumes containing many vortex lines:[5]

$$\frac{\partial \boldsymbol{v}_s}{\partial t} + \boldsymbol{\nabla}\left(\mu + \frac{v_s^2}{2}\right) = \boldsymbol{v}_s \times \boldsymbol{\omega} + \alpha' \boldsymbol{\omega} \times (\boldsymbol{v}_s - \boldsymbol{v}_n) + \alpha\, \hat{\boldsymbol{\omega}} \times [\boldsymbol{\omega} \times (\boldsymbol{v}_s - \boldsymbol{v}_n)]. \quad (1)$$

Here $\boldsymbol{v}_n$ is the flow imposed on the normal component, $\boldsymbol{\omega} = \boldsymbol{\nabla} \times \boldsymbol{v}_s$, $\hat{\boldsymbol{\omega}}$ is a unit vector in the direction of $\boldsymbol{\omega}$, μ is the chemical potential, α and α' are the dissipative and reactive mutual friction coefficients, respectively. The vortex line tension is neglected. Applying simple dimensional comparison of the magnitudes of the dissipative term (containing α) to the inertial terms in Eq. (1), similar to how one introduces the Reynolds number in the classical Navier-Stockes equation, one arrives to the conclusion[2,6] that the character of the flow is controlled by the ratio of the mutual friction coefficients $q = \alpha/(1 - \alpha')$: Turbulence occurs only if $q < q_c \sim 1$. The transition from laminar to turbulent dynamics becomes velocity-independent in the range of validity of Eq. (1) (which includes the requirement for a sufficiently large flow velocity). This is seen from the scale invariance of Eq. (1): If $\boldsymbol{v}_s(\boldsymbol{r}, t)$

is the solution of this equation (and of the continuity equation $\mathrm{div}\, \boldsymbol{v}_\mathrm{s} = 0$) for a given imposed flow $\boldsymbol{v}_\mathrm{n}$, then $\lambda \boldsymbol{v}_\mathrm{s}(\boldsymbol{r}, \lambda t)$ is the solution for the scaled imposed flow $\lambda \boldsymbol{v}_\mathrm{n}$.

In this report we extend the investigation of the transition between regular and turbulent vortex dynamics in ^{3}He-B to the pressure range from zero up to the solidification pressure and examine the question whether the transition to turbulence is controlled by a single universal value q_c at all conditions.

2. EXPERIMENT

A detailed account of the experimental techniques, including the injection of the seed vortex loops and the NMR detection, is given in Ref. 6. Here we present a brief summary. The ^{3}He sample is contained in a cylindrical container with radius $R = 3\,\mathrm{mm}$ and height 11 cm. At mid-height there is a barrier magnet which provides a magnetic field to stabilize the A phase at all temperatures. The lower and upper sections of the sample remain in the B phase. Two NMR detection coils are installed in these sections close to the top and bottom ends of the sample. From the NMR measurements the number of vortex lines within the coil can be determined.

In the absence of the A phase the B phase in our experiments remains vortex-free in rotation up to some container-specific critical angular velocity. Its value is not in good control but for the containers used in the present work it exceeds $2\,\mathrm{rad/s}$ at $T < 0.8\,T_\mathrm{c}$. When the A phase is present in the middle of the sample the seed vortex loops are injected into the B phase at a well defined and reproducible Ω as a result of the Kelvin-Helmholtz (KH) instability of the AB interface.[7] This velocity is a well-understood smooth function of T, P and of the current in the barrier magnet I_b. The circulation carried by the initial B-phase vortices comes from the vortex layer which covers the AB interface. In the layer vorticity is arranged in a regular manner, with vortices aligned radially and parallel to the AB interface.[8] Thus one may expect that the configuration of the seed vortices is reasonably well reproducible with one end of each vortex sticking out of the AB interface and the other end perpendicular to the outer wall of the sample. Our measurements indicate that the size of a seed vortex is about $0.4\,\mathrm{mm}$.[8] The injection parameter, which is not in good control, is the number of the seed vortices, produced by one instability event. This number has a rather wide distribution in the range 3–30 vortices,[6] with the average value of about 10. The reason for such a wide variation is presently not known.

The result from the expansion of the seed vortices along the B-phase column is observed when they reach the NMR coils. A few vortices (in the case of regular expansion) and an array with many vortex lines (in the case

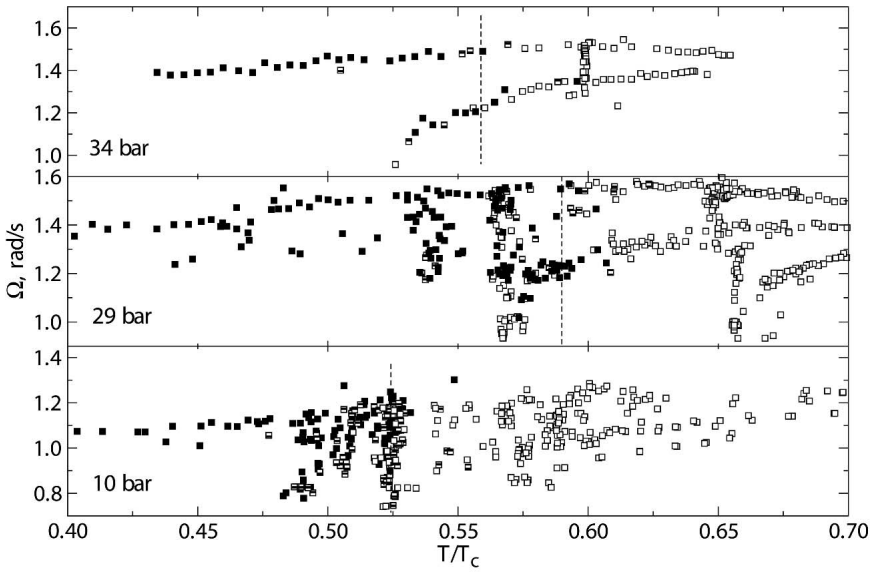

Fig. 1. Transition between regular (open squares) and turbulent (filled squares) vortex dynamics as a function of temperature at three pressures. The dashed vertical lines represent the average values $T_{\rm t}$ of the distributions in Fig. 2.

of turbulent expansion) are easily distinguished at $T > 0.4\,T_{\rm c}$. The two B-phase sections of the sample present two independent experimental volumes. Their simultaneous measurement improves the statistics of the results.

3. RESULTS

Figs. 1–4 summarize the transition from regular to turbulent dynamics with decreasing temperature and trace the transition as a function of Ω, T, and P. Here Ω is the critical velocity for the KH instability, at which vortices have been injected in the flow. In most cases the B phase has been completely vortex-free before the injection and thus the flow in the sample is $\boldsymbol{v}_{\rm n} - \boldsymbol{v}_{\rm s} = \boldsymbol{\Omega} \times \boldsymbol{r}$. The data have been measured along continuous trajectories, either by scanning temperature at constant barrier current $I_{\rm b}$ or by scanning $I_{\rm b}$ at constant T. These trajectories are not emphasized in the plots, instead the data have been classified in regular (open symbols) or turbulent (filled symbols) events, to highlight the transition separating them.

On the basis of the data in Fig. 1 (which is plotted in a different way in the later figures) we conclude that the transition is independent of the

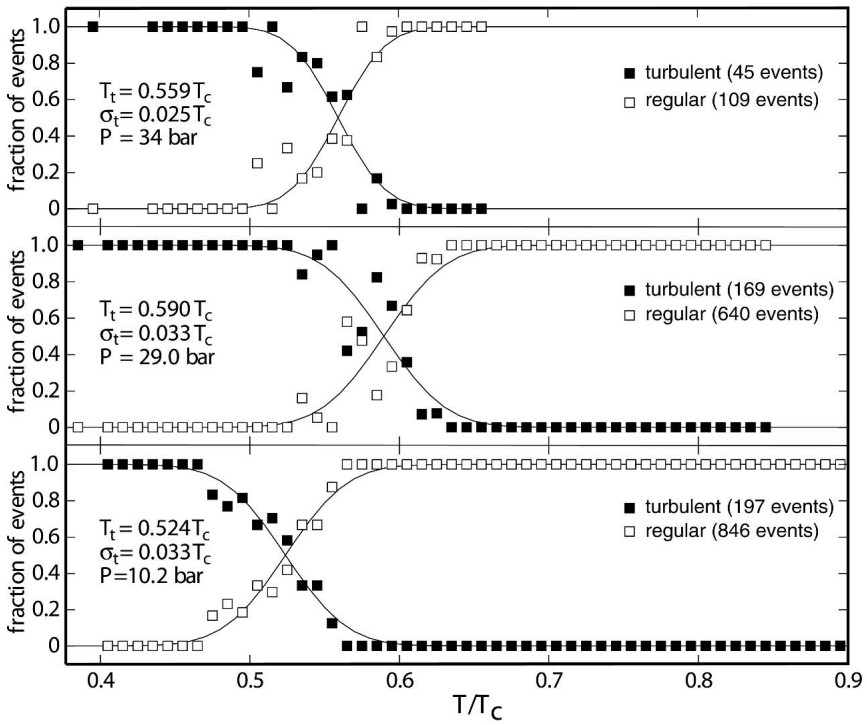

Fig. 2. Probability for a vortex expansion event to be regular (open squares) or turbulent (filled squares) as a function of temperature at three pressures. The probabilities are calculated by arranging events from Fig. 1 as a function of temperature in bins of $0.01\,T_c$ width at the three pressures. The continuous curves are fitted normal cumulative distribution functions with the average transition temperature T_t and dispersion σ_t, as given in each panel.

velocity Ω, if compared with the width of the transition. This agrees with expectations based on the scale invariance of the equation (1). This conclusion is valid for high velocities, while low velocities much below the present range of $\sim 1\,\mathrm{rad/s}$ should be checked separately.

Other features demonstrated by Fig. 1 are that the transition has a certain width and that the transition temperature might depend on pressure. To quantify these features the probabilities to oberve regular and turbulent events are plotted in Fig. 2 as a function of temperature for the 3 pressures. Each of these distributions is fitted with a normal cumulative distribution function with average value T_t and dispersion σ_t as fitting parameters. This

function has been chosen as a simple way to obtain numerical values for the average transition temperature and its width. We do not claim that the usage of the Gaussian distribution has a solid physical reason.

For all 3 pressures the transition half-width is found to be around $\sigma_t \approx 0.03\,T_c$. We believe that fluctuations in the injection process are the main cause for the widths in Fig. 2. It appears probable that at higher temperatures only some of the initial configurations of vortices (say, the ones with a larger number of initial loops) will evolve to a turbulent network. As the temperature decreases more of the different initial configurations become unstable towards turbulence. This picture is supported by comparison with experiments on turbulence initiated by neutron absorption in ^{3}He-B.[10] KH injection which we use in this work produces almost always more than 3 vortex loops, while in the neutron absorption the production of 1–2 vortex loops is the most common case. As has been observed in Ref. 10, the transition to turbulence becomes wider towards lower temperatures if it is initiated by neutron absorption: Even at $0.45\,T_c$ regular events are still rather common. Numerical simulations of vortex dynamics[11] also demonstrate that at intermediate temperatures a single vortex loop in the rotating container may initiate turbulence or may not, depending on the initial configuration. In classical liquids a similar situation occurs in the transition from laminar to turbulent flow in a pipe: There is a critical amplitude of perturbation which triggers the transition and this amplitude scales inversely proportional to the flow velocity.[12]

The dependence of the average transition temperature T_t on pressure is shown in Fig. 3. The data from Fig. 2 have been augmented by the measurements at $P = 0$. At zero pressure we have not observed the turbulence at $T > 0.45\,T_c$ at rotation velocities 0.5 – 0.7 rad/s. On the other hand, turbulent vortex tangles have been observed at $T < 0.2\,T_c$ using vibrating wires.[3] Combining all the data, we conclude that there is a pressure dependence of the transition to turbulence on the T/T_c scale.

When inspecting Fig. 3 one should keep in mind that from the three sets of measurements in Fig. 1 more effort was invested in the temperature calibration and data taking of the runs at 29.0 and 10.2 bar pressures, while the 34 bar measurements were more qualitative in character. Thus, a non-monotonous dependence of T_t/T_c on pressure cannot be claimed. It may simply be an artefact of the small amount of data measured at 34 bar. However, we note here an interesting phenomenon, which might affect the transition to turbulence at high pressures. As indicated by the dashed line in Fig. 3 there is a first-order transition[9] in the vortex core structure between a non-axisymmetric core at low T, P and an axisymmetric core at high T, P. The structure of the core affects the mutual friction parameters and the

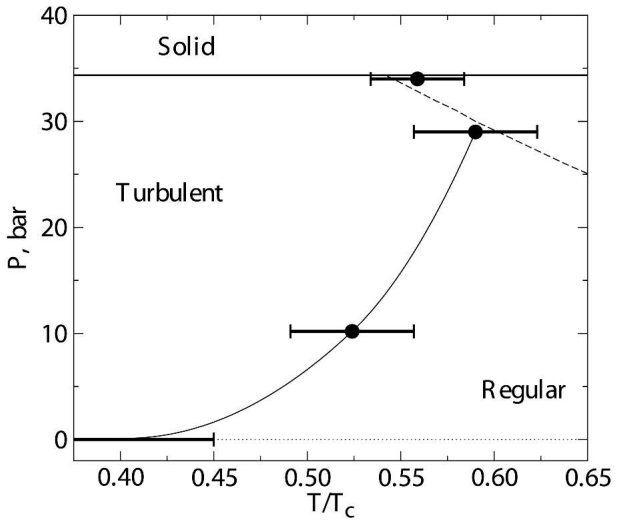

Fig. 3. Phase diagram of turbulence in ^{3}He-B. The points for 10, 29 and 34 bar represent the middle of the transition T_t from regular dynamics at higher temperatures to turbulent dynamics at lower temperatures, as determined from the distributions in Fig. 2. The error bars indicate the width of the transition σ_t as determined from these distributions (and do not indicate the uncertainty in temperature). At zero pressure the error bar indicates the unexplored region where the transition to turbulent dynamics should occur. The solid line is a guide for the eye. The dashed line shows the transition in vortex core structure[9] which leads to a discontinuity in the mutual friction coefficients.[4]

dissipation associated with a non-axisymmetric vortex is larger.[4] It is therefore possible that there is a kink in the $T_t(P)$ dependence at the transition between the two core structures.

What is the reason for the pressure dependence of the transition to turbulence? Eq. (1) suggests that the transition is controlled by the ratio of the mutual friction parameters, $q = \alpha/(1-\alpha')$. Thus it is instructive to plot our data as a function of q. Unfortunately, the precise measurements of $q(T,P)$ are available only for two pressures, 10 and 29 bar.[4] Our data for these pressures from Fig. 1 have been repeated as a function of q in Fig. 4. Generally speaking, the transition takes place when $q \sim 1$. However, a critical value of q is not universal: the transition moves to larger q as a function of pressure. Can we be sure that the difference in q values for the transitions in Fig. 4 is experimentally significant? First we note that the

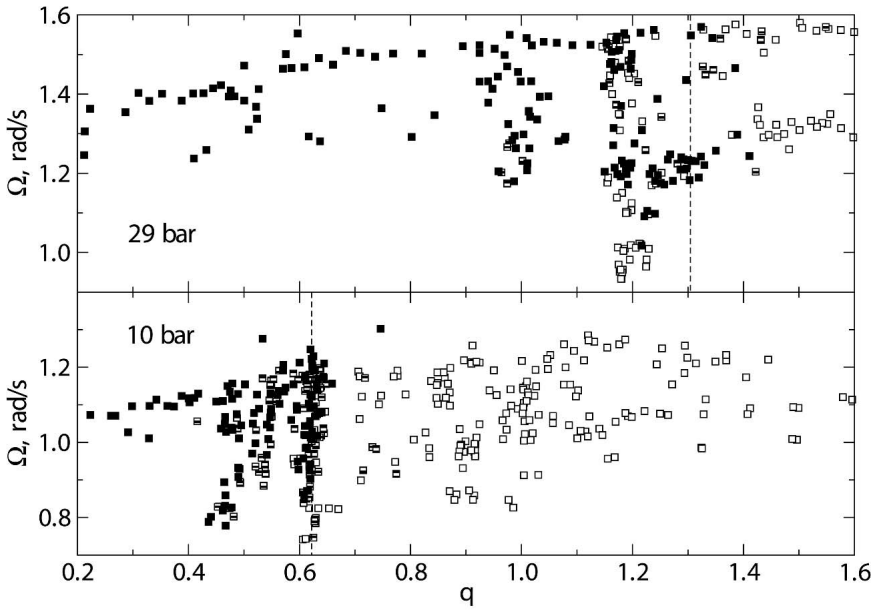

Fig. 4. Transition between regular (open squares) and turbulent (filled squares) vortex dynamics as a function of the ratio of the mutual friction coefficients $q = \alpha/(1-\alpha')$ at the two pressures where $q(T,P)$ was measured in Ref. 4.

mutual friction coefficient α can be measured in our experiment in situ using the time-of-flight technique described in Refs. 13 and 6. Such measurements give values of α which agree with Ref. 4 both at 29 and 10 bar pressure. Thus there is no systematic error, for example, in the temperature scales. The scatter of the data points in Ref. 4 gives an uncertainty in q of about ± 0.04 at $P = 10\,\mathrm{bar}$. For $P = 29\,\mathrm{bar}$ the situation is more difficult to estimate, since there exists an additional scatter due to the presence of two different types of vortices around $0.6\,T_\mathrm{c}$. The possible range of q values at the transition temperature is from $q \approx 1.13$ for the high-temperature axisymmetric vortex to $q \approx 1.72$ for the low-temperature non-axisymmetric vortex (the same type which occurs at 10 bar). Thus, even with these uncertainties, the critical values of q for the two pressures in Fig. 4 remain well separated.

Thus, whether the vortex dynamics is turbulent or regular in character, indeed strongly depends on the magnitude of mutual friction damping. However the simple classification on the basis of the value of q, as suggested in Ref. 2, agrees with the experiment only as an order of magnitude estimation. To explain the pressure dependence of the transition to turbulence

presented here more experimental and theoretical work is required. At the moment we can only speculate about possible reasons.

First, the analysis of Eq. (1) may not be completely correct. This equation includes two parameters, α and α', and the transition may depend on their values in a more complicated way than the simple ratio q. Second, the equation itself may not be fully applicable to the experimental situation. In particular, in the process of coarse-graining the mutual friction force over volumes containing many vortex lines the values of the mutual friction coefficients may become renormalized from their single-vortex values measured in Ref. 4. Next, the properties of the injection of the seed loops may depend on pressure in such a way that the initial configurations of vortices become less favourable for initiating the turbulence with decreasing pressure. However, in the latter case one would expect that the width of the transition will also increase, similar to the turbulence induced by neutron absorption,[10] which is not observed in Fig. 2.

At present it is assumed that one vital precondition is required to start turbulence: it is the Kelvin-wave instability[14] of a vortex line. It provides the mechanism by which quantized vorticity starts to multiply even from one single vortex loop which is injected in the rotating vortex-free counterflow. The Kelvin-wave instability switches on when some section of the vortex loop becomes oriented along the flow. In this part of the vortex filament a helical Kelvin wave starts to grow in amplitude. The wave develops into loops which reconnect to form separated vortex rings. These rings provide the beginning of the evolving network. The triggering and development of the Kelvin-wave instability is significantly affected by the vortex line tension, which has so far been neglected here. The tension depends, although only logarithmically, on the vortex core size, which decreases in ^{3}He-B by almost an order of magnitude from zero to melting pressure. This might also influence the transition to turbulence.

The final complication, which we note here, concerns the role of the magnetic field. Close to the AB interface, where the seed vortex loops are injected, the magnetic field is high and distorts the superfluid gap in the B phase as well as the structure of the vortex core. These are the parameters which directly determine the magnitude of the mutual friction coefficients.[15] If the turbulence is initiated in the immediate vicinity of the original position of the seed loops then the transition to turbulence might also be affected by the pressure and temperature dependent magnetic field $H_{\rm AB}$. The measurements with neutrons[10] are free from these complications but the transition in this case is wide, as has been explained above, and the presently available results do not allow to pinpoint the critical q value with enough accuracy to judge its pressure dependence.

4. CONCLUSIONS

We have described the first measurements on the phase diagram of turbulence in ^{3}He-B: (i) A wide regime of mutual friction damping has been examined as a function of temperature, which is not easily accessible in the case of ^{4}He-II. Mutual friction proves to control the character of vortex motion in superfluid hydrodynamics: when $\alpha/(1-\alpha') \gtrsim 1$ the number of vortex lines is a conserved quantity, while in the opposite case, $\alpha/(1-\alpha') \lesssim 1$, the vortex number rapidly proliferates through turbulence. It is known from ^{4}He-II that mutual friction can help to sustain turbulence by blowing up Kelvin-wave perturbations on vortex loops and it also can damp turbulent motion at certain length scales.[1,16] From ^{3}He-B we now find that high mutual friction can totally suppress turbulence. (ii) The transition to turbulence is not marked by a unique value of the mutual friction ratio $q = \alpha/(1-\alpha')$; with increasing pressure the transition moves to higher q. (iii) Turbulence is prominently concentrated in the low-temperature, high-velocity, and high-pressure corner of the ^{3}He-B phase diagram. At higher flow velocities the transition between regular and turbulent dynamics is velocity independent, the width of the transition regime is narrow and centered in the temperature interval $0.5 - 0.6\,T_c$, depending on pressure.

Acknowledgments. We thank C. Barenghi, R. Blaauwgeers, G. Eska, D. Kivotides, N.B. Kopnin, L. Skrbek, M. Tsubota, W.F. Vinen, and G.E. Volovik for valuable discussions. This work has benefited from the EU-IHP ULTI-3 visitor program and the ESF programs COSLAB and VORTEX.

REFERENCES

1. W.F. Vinen and J.J. Niemela, *J. Low Temp. Phys.* **128**, 167 (2002).
2. A.P. Finne et al., *Nature* **424**, 1022 (2003).
3. S.N. Fisher et al., *Phys. Rev. Lett.* **86**, 244 (2001).
4. T.D.C. Bevan et al., *J. Low Temp. Phys.*, **109**, 423 (1997).
5. E.B. Sonin, *Rev. Mod. Phys.* **59**, 87 (1987).
6. A.P. Finne et al., *J. Low Temp. Phys.*, November (2004).
7. R. Blaauwgeers et al., *Phys. Rev. Lett.* **89**, 155301 (2002).
8. R. Hänninen et al., *Phys. Rev. Lett.* **90**, 225301 (2003).
9. J.P. Pekola et al., *Phys. Rev. Lett.* **53**, 584 (1984).
10. A.P. Finne et al., *J. Low Temp. Phys.*, June (2004).
11. R. Hänninen, A. Mitani, and M. Tsubota, *J. Low Temp. Phys.*, this issue.
12. B. Hof et al., *Phys. Rev. Lett.* **91**, 244502 (2003).
13. A.P. Finne et al., *J. Low Temp. Phys.* **134**, 375 (2004).
14. R.M. Ostermeier and W.I. Glaberson, *J. Low Temp. Phys.* **21**, 191 (1975).
15. N.B. Kopnin, *Theory of Nonequilibrium Superconductivity* (Oxford University Press, 2001), p. 271.
16. D.C. Samuels and D. Kivotides, *Phys. Rev. Lett.* **83**, 5306 (1999).